HYDROCODE SIMULATION OF THE TRANSITION FROM CENTRAL PEAK TO PEAK-RING CRATER MORPHOLOGY FOR THE MOON. C. Milbury[1] , B. C. Johnson[1] and H. J. Melosh[1], [1]Department of Earth, Atmospheric, and Planetary Science, Purdue University, 550 Stadium Mall Drive, Hampton Hall, Room 3233, West Lafayette, IN 47907 (cmilbury@purdue.edu).

Introduction: The observed transition from simple to complex crater morphology is driven by gravitational collapse of the transient crater. The mechanism that causes the transition from complex to peak-ring crater morphology is still debated. There are two dominant models that have been proposed to explain this transition in crater morphology. Both the central peak collapse model [1, 2] and the nested melt cavity model [3, 4] predict the observed morphological features and depth to diameter ratios. By calculating peak and peak ring volumes, Bray et al. [5] showed that the data tend to support peak-ring formation by collapse of the central peak.

In this study, we systematically investigate this change in crater morphology using the iSALE hydrocode and varying the Acoustic Fluidization (AF) parameters over a broad range of values. We will identify where melt is produced and calculate the melt volume so these can be compared with the nested melt cavity model predictions.

Background: Melosh [6] was the first to put forward the idea of AF, which is the temporary behavior of fractured rock as a viscous fluid. It is triggered by intense, short-wavelength vibrations within the target and it occurs mostly within the crater collapse phase of the impact process. Wünnemann & Ivanov [7] carried out simulations using the AF model to match the observed depth to diameter ratios over a range of crater sizes for the Moon, Earth, and Venus.

Methodology: We use the following model parameters in our simulations: an equation of state granite crust and a dunite mantle, an impact velocity of 17 km/s, a lunar gravity of 1.62 m/s^2, a target heat flow of 18 mW/m^2, and a melt temperature of 1373 K. We systematically vary the AF parameters, Υ_T and Υ_η, to understand how they affect crater morphology. Υ_T is a scaling factor related to the decay time and controls the amount of time the target is subject to AF, and Υ_η is the viscosity-scaling parameter [7].

For each model run, the crater depth, diameter, and central peak height and width are compared to those determined by Kalynn et al. [8] for lunar complex craters using topographic data. The impactor size will be increased such that the characteristics for larger impact structures can be examined. Figure 1 shows the temperature profile 700 s after impact with a 7 km diameter dunite impactor. These will be compared with specific craters on the Moon, and the gravity signature associated with these craters will also be modeled using data from NASA's Gravity Recovery And Interior Laboratory (GRAIL) mission.

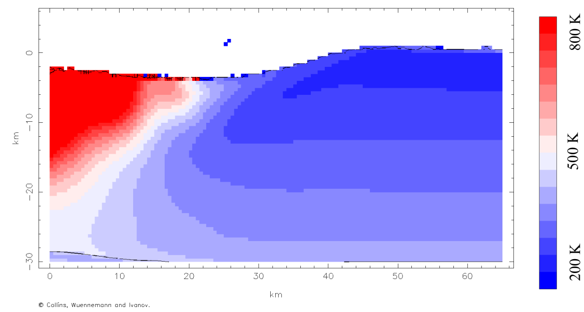

Figure 1. The temperature profile 700 s after impact.

Discussion: Understanding this observed change in crater morphology has implications beyond the Moon. The transition from central peak to peak-ring craters and these types of craters is observed throughout the solar system. Alexopoulos & McKinnon [9] documented this transition for Venusian craters using Arecibo and Venera radar images and Magellan radar data. Since the MESSENGER mission arrived at Mercury, an increasing number of complex and peak-ring craters have been identified [10]. Nycz & Hildebrand [11] used Viking and Mars Orbiter Camera images to identify and classify 680 impact structures on Mars. They showed a size and morphological progression similar to that of [9]. Multiringed basins are not unique to terrestrial bodies; they have been observed on Jupiter's icy moons [12].

Investigating this transition is clearly important and it may help to shed new light into the cratering process and the mechanism that causes this tobserved transition in crater morphologies.

References: [1] Morgan, J. V. et al (2000) *EPSL, 183*, 347-354. [2] Collins, G. S. et al. (2002) *Icarus, 157*, 24-33. [3] Head J. W. et al (2010) *GRL, 37*, L02203. [4] Baker D. M. et al (2011a) *Icarus, 214*, 377–393. [5] Bray V. J. et al. (2012) *GRL, 39*, L21201. [6] Melosh (1979) *JGR, 84*, 7513-7520. [7] Wünnemann K. and Ivanov B. A. (2003) *PSS, 51*, 831-845. [8] Kalynn J. et al. (2013) *GRL, 40*, 38-42. [9] Alexopoulos J. S. and McKinnon W. B. (1994) *SPGSA, 293*, 29-50. [10] Baker D. M. et al., (2011b) *PSS, 59*, 1932-1948. [11] Nycz J. C. and Hildebrand A. R. (2003) *MPSA*, #5255. [12] Schenk P. M. and McKinnon W. B. (1987) *Icarus, 72*, 209-234.